

Synthesis, antimicrobial activity and molecular modeling of cobalt and nickel complexes containing the bulky ligand: *bis*[*N*-(2,6-diisopropylphenyl)imino] acenaphthene

Usama El-Ayaan ^{a,*}, Alaa A.-M. Abdel-Aziz ^b

^a Department of Chemistry, Faculty of Science, Mansoura University, Mansoura 35516, Egypt

^b Department of Medicinal Chemistry, Faculty of Pharmacy, Mansoura University, Mansoura 35516, Egypt

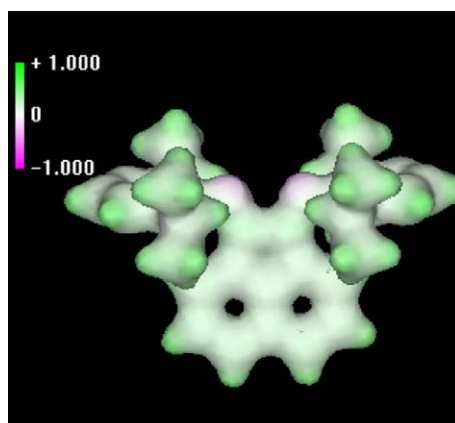
Received 24 June 2005; accepted 28 June 2005

Available online 29 August 2005

Abstract

Two cobalt and two Nickel complexes of *bis*[*N*-(2,6-diisopropylphenyl)imino]acenaphthene (**Pr-BIAN**) ligand, have been synthesized. These complexes, namely [Co(Pr-BIAN)Cl₂] **1**, [Co(OAc)₂(Pr-BIAN)₂](ClO₄) **2**, [Ni(Pr-BIAN)(NO₃)₂] **3** and [Ni(Pr-BIAN)₂](ClO₄)₂ **4**, were characterized by elemental analyses, molar conductance, spectral (IR, UV–Visible and NMR) and magnetic moment measurements. In these complexes the geometries about the metal center are significantly different. While for complexes **2** and **3** an octahedral structure is proposed, in complex **4**, square-planar coordination with an almost perfect planar arrangement of two **Pr-BIAN** ligands around the nickel center is suggested. In **1**, two imine nitrogen atoms of **Pr-BIAN** and two chloride atoms are coordinating in a tetrahedral fashion around the cobalt center. Molecular mechanics (MM+) and semiempirical molecular orbital calculations have been performed for the most biologically active complex **1** and its free ligand **Pr-BIAN** and compared with inactive ligand *bis*[*N*-(*p*-tolylphenyl)imino]acenaphthene **6**, to get insight into their molecular structures and to learn more about their stable molecular conformations.

© 2005 Elsevier SAS. All rights reserved.



Keywords: Nickel complexes; *bis*[*N*-(2,6-diisopropylphenyl)imino] acenaphthene; **Pr-BIAN**

* Corresponding author. Tel.: +20 10 589 4252; fax: +20 50 224 6781.

E-mail address: usama@mans.edu.eg (U. El-Ayaan).

1. Introduction

Schiff Bases are characterized by the $-N=CH-$ (imine) group which is important in elucidating the mechanism of transamination and rasemination reaction in biological system [1,2]. Although many Schiff bases are known to be active against a wide range of micro-organisms, for example; *C. albicans*, *E. coli*, *S. aureus*, *B. polymxa*, *T. gypseum*, *E. graminis* and *P. viticola*, antibacterial activity has been studied more than antifungal activity, since bacteria are usually more resistant to antibiotics through biochemical and morphological modifications [3,4]. Moreover, the incorporation of transition metal into Schiff bases enhances the biological activity of the ligand and decreases the cytotoxic effects of both the metal ion and ligand on the host [5].

Recently, special attention focused on the catalytic reactivity of late transition metals, like rhodium, palladium and platinum and their compounds containing rigid bidentate ligands, such as *bis*(*N*-arylimino)acenaphthene (Ar-BIAN) [6–9]. These Ar-BIAN ligands are regarded as a diimine containing two conjugated imine functions. These two exocyclic imines, which are not part of the heterocyclic ring system, are leading to better σ -donating and better π -accepting properties. This property allows the ligand to stabilize both the higher and lower oxidation states of the metal ions. In addition,

the rigidity of the acenaphthene backbone forces the imine *N*-atoms to remain in a fixed *cis* orientation, favoring a chelating coordination to a metal center.

This paper contains the synthesis and characterization of the complexes $[Co(Pr-BIAN)Cl_2]$ **1**, $[Co(OAc)_2(Pr-BIAN)_2](ClO_4)_2$ **2**, $[Ni(Pr-BIAN)(NO_3)_2]$ **3** and $[Ni(Pr-BIAN)_2](ClO_4)_2$ **4**. *Bis*[*N*-(2,6-diisopropyl phenyl) imino] acenaphthene **Pr-BIAN** (Fig. 1) was synthesized from acenaphthenequinone and 2,6-diisopropylaniline as previously reported [10]. The antimicrobial screening of these complexes and the free ligand against different bacterial and fungal species, compared with *bis*[*N*-(2,4,6-trimethylphenyl) imino] acenaphthene **5** [11] and *bis*[*N*-(*p*-tolylimino)] acenaphthene **6** have been also reported [12].

2. Results and discussion

Two, cobalt and two, nickel complexes containing rather bulky Pr-BIAN ligand have been synthesized according to the following synthetic method:

For (**1**), $CoCl_2 \cdot 6H_2O + Pr-BIAN$ (in EtOH/HOAc) $\rightarrow [Co(Pr-BIAN)Cl_2]$.

For (**2**), $Co(ClO_4)_2 \cdot 6H_2O + 2Pr-BIAN + (in HOAc/w MeOH/CHCl_3 + O_2) \rightarrow [Co(OAc)_2(Pr-BIAN)_2](ClO_4)_2$.

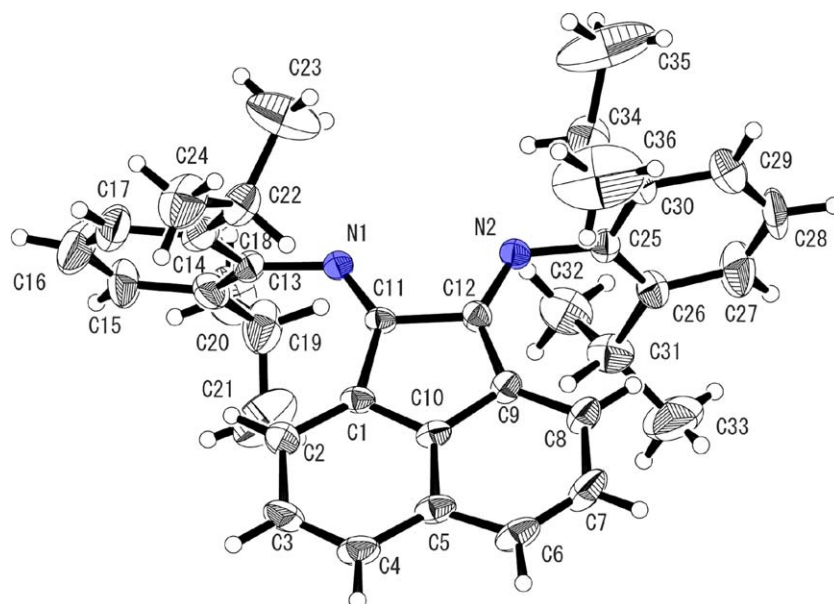


Fig. 1. Structure of the ligand (**Pr-BIAN**).

Table 1
Antimicrobial screening results of the tested compounds at 1 mg ml⁻¹ and their CLogP*

Compound number	Clog P	<i>P.aeruginosa</i>	<i>E. coli</i>	<i>S. aureus</i>	<i>B. subtilis</i>	<i>C. albicans</i>
Pr-BIAN	12.3	12	18	15	na	14
5	9.6	10	16	13	na	10
6	7.6	na	Na	na	na	na
1		14	22	17	na	16
2		12	19	16	na	15
4		11	18	14	na	13

* Ref. [25]. Strong activity (> 14 mm), moderate activity (9–14 mm), weak activity (5–8 mm), na; no activity (inhibition zone < 5 mm), Solvent: DMSO (4 mm).

Table 2

Analytical, physical and Infrared (cm^{-1}) data of complexes

Compound		Found (Calc.) %			Λ_m $\Omega^{-1}\text{cm}^2\text{mol}^{-1}$		IR (cm^{-1})		
Empirical formula	F.Wt	C	H	N	AN	NM	$\nu(\text{C}=\text{N})$	$\nu(\text{ClO}_4^-)$	$\nu(\text{NO}_3^-)$
$[\text{Co}(\text{Pr-BIAN})\text{Cl}_2]$, $\text{C}_{36}\text{H}_{40}\text{Cl}_2\text{CoN}_2$	630.5	69.27 (68.58)	6.67 (6.39)	4.36 (4.44)	27	5	1646, 1620		
$[\text{Co}(\text{OAc})_2(\text{Pr-BIAN})_2](\text{ClO}_4)$, $\text{C}_{76}\text{H}_{86}\text{ClCoN}_4\text{O}_8$	1277.9	70.01 (71.4)	6.68 (6.78)	4.59 (4.38)	200	100	1670, 1633	1116, 621	
$[\text{Ni}(\text{Pr-BIAN})(\text{NO}_3)_2]$, $\text{C}_{36}\text{H}_{40}\text{N}_4\text{NiO}_6$	683.4	62.85 (63.3)	5.86 (5.90)	8.15 (8.20)	57	25	1656, 1627		1766, 1725
$[\text{Ni}(\text{Pr-BIAN})_2](\text{ClO}_4)_2$, $\text{C}_{72}\text{H}_{80}\text{Cl}_2\text{N}_4\text{NiO}_8$	1259	69.37 (68.69)	6.73 (6.4)	4.66 (4.45)	316	185	1668, 1634	1116, 621	

For **(3)**, $\text{Ni}(\text{NO}_3)_2 \cdot 6\text{H}_2\text{O} + \text{Pr-BIAN}$ (in EtOH) $\rightarrow [\text{Ni}(\text{NO}_3)_2(\text{Pr-BIAN})]$.

For **(4)**, $\text{Ni}(\text{ClO}_4)_2 \cdot 6\text{H}_2\text{O} + 2\text{Pr-BIAN}$ (in HOAc) $\rightarrow [\text{Ni}(\text{Pr-BIAN})_2](\text{ClO}_4)_2$.

Analytical, physical and infrared data of complexes are listed in Table 2. The complexes are quite stable in air and soluble in common organic solvents. The molar conductivities of complexes (Table 2) were measured in acetonitrile (AN) and in nitromethane (NM). These measurements indicate 1:1 electrolytic type for complex **2** and 2:1 for complex **4**. This confirms that ClO_4^- anions are acting as counter ions and are not coordinating to the metal center. In complexes **1** and **3**, the molar conductivity values are in the range of non-electrolytes [15].

2.1. IR spectra of complexes

Bands assigned to $\text{C}=\text{N}$ stretching vibrations of the free ligand were observed in the $1642\text{--}1671\text{ cm}^{-1}$ range. These bands are shifted to lower wave numbers in the complexes, which is a criterion of the coordination of both diimine nitrogen atoms of the **Pr-BIAN** ligand to the metal ion (Table 2). It is known that IR spectra may be used efficiently to distinguish the mode of nitrate anion coordination [16]. Fukuda et al. studied carefully such behavior and found that: [17–19] (1) ionic nitrate appear as one weak band ($\nu_1\text{--}\nu_4$ combination band) near 1750 cm^{-1} , (2) monodentate nitrate: weak splitting (less than 20 cm^{-1}) of the band in the $1700\text{--}1800\text{ cm}^{-1}$ region, (3) bidentate nitrate: strong splitting (more than 20 cm^{-1}) in the same region. In this study, the IR spectrum of complex **3** shows two bands at 1766 and 1725 cm^{-1} indicating the bidentate coordination of the nitrate groups. In complexes **2** and **4**, a sharp band observed at 621 cm^{-1} (antisymmetric bend), and a strong band at 1116 cm^{-1} (antisymmetric stretch) suggest uncoordinated perchlorate anions [20].

Generally, it is known that the aromatic rings with three adjacent carbon–hydrogen bonds show strong bands in the $810\text{--}750\text{ cm}^{-1}$ region due to out-of-plane CH deformation vibrations [21]. Their position is determined almost wholly by their location on the ring rather than by the nature of the substituent and, with certain limitations, they provide an excellent method for recognition of the type of substitution. The very high intensity and sensitivity of these characteristic bands

in this region make them particularly well suited for quantitative work, too. The splitting of these out-of-plane CH deformation vibrations bands in the $850\text{--}750\text{ cm}^{-1}$ region of the complexes can be considered as a sign of the coordination of two **Pr-BIAN** ligands to the metal ion [22]. In the IR spectra, splitting was observed in complexes **2** and **4** while no such splitting was observed in the case of **1** and **3** complexes where only one ligand molecule is coordinated.

2.2. Electronic spectra of complexes

The electronic spectra of complexes were measured in the solid-state and in solution using a variety of solvents [dichloroethane (DCE), acetonitrile (AN) and chloroform (CHCl_3)]. All solution spectra of the complexes **1–4** are very similar to the corresponding solid-state spectra. The band positions and magnetic moments of complexes are given in Table 3. The electronic spectra of complex **1** exhibit a multiple absorption in the visible region. A strong band observed at 719 nm can be assigned to the ($^4\text{A}_2 \rightarrow ^4\text{T}_1(\text{P})$) transition, typical for tetrahedral $\text{Co}(\text{II})$ complexes. The green color as well as the magnetic moment of 4.9 B.M. , are further indication for the tetrahedral geometry. The electronic spectra of the low spin $\text{Co}(\text{III})$ complex namely, $[\text{Co}(\text{OAc})_2(\text{Pr-BIAN})_2](\text{ClO}_4)$ exhibit two bands observed at 570 and 470 nm , which can be assigned to $^1\text{A}_{1g} \rightarrow ^1\text{T}_{1g}$ and $^1\text{A}_{1g} \rightarrow ^1\text{T}_{2g}$ transitions, respectively, typical for octahedral $\text{Co}(\text{III})$ geometry [23]. The electronic spectra of the hexa-coordinated nickel (II) complex, $[\text{Ni}(\text{Pr-BIAN})(\text{NO}_3)_2]$ exhibit three bands observed at 990 , 620 and 390 nm , which can be assigned to $^3\text{A}_{2g} \rightarrow ^3\text{T}_{2g}$, $^3\text{A}_{2g} \rightarrow ^3\text{T}_{1g}$ and $^3\text{A}_{2g} \rightarrow ^3\text{T}_{1g}(\text{P})$ transitions, respectively, typical for octahedral $\text{Ni}(\text{II})$ geometry [21]. The magnetic moment of 3.2 B.M. is additional evidence for the octahedral geometry. The electronic spectra of the nickel complex, $[\text{Ni}(\text{Pr-BIAN})_2](\text{ClO}_4)_2$ (Fig. 2), exhibit a single band at 530 nm typical for square-planar $\text{Ni}(\text{II})$ complexes. A second more intense band observed at 470 nm is assigned as charge transfer band.

2.3. NMR spectra of the ligand and the complexes **2** and **4**

^1H and ^{13}C NMR data of the free ligand and the complexes **2** and **4** are listed in Tables 4 and 5, respectively. In the free ligand, the low-frequency doublet observed at 6.64 ppm

Table 3
Magnetic moment and electronic bands of complexes (1)–(4)

Compound	Wavelength (nm)				μ_{eff} (B.M.)
	(Molar extinction coefficient, ϵ , L mol ⁻¹ cm ⁻¹)				
	Solid	DCE	AN	CHCl ₃	
Complex (1)	719	719 (405), 661 (204), 595 (132)	720 (409), 663 (210), 590 (140)	722 (412), 660 (202), 597 (146)	4.90
Complex (2)	570, 470	567 (1903), 453 (6909), 363 (sh)	563 (1300), 440 (8010), 360 (sh)	565 (1087), 429 (5399), 363 (sh)	diam
Complex (3)	990, 620, 390	1018(12.8), 612(42.35), 393(2106)	996(16.27), 617(27.54), 393(1435.6)	1011(15.14), 617(51.38), 396(1913)	3.20
Complex (4)	530, 470	540(1470), 453 (5280), 360(5480)	545(930), 440(5700), 360(6180)	540(820), 430 (1380), 370(2500)	diam

diam = diamagnetic.

is assigned to H2 (see Fig. 1, the number of the H atom corresponds to the attached C atom), which is anisotropically shielded by the aromatic substituent that is oriented out of the naphthalene plane. This assignment is confirmed by comparison with the ¹H NMR data of acenaphthenequinone and en-BIAN (en = ethylenediamine), neither of which exhibits the shielding effect of an aromatic substituent on the imine nitrogen atom and give resonances of H2 at 8.0 and 7.9 ppm, respectively. Furthermore, the observed shift of the resonance of H2 to lower frequency upon *ortho* substitution (*o,o'*-diisopropyl groups) on the imine N atoms agrees with this assignment, as *ortho* substituents are expected to lead to a more perpendicular orientation of the aromatic group and a concomitant increased anisotropic shielding of H2. These results indicate that the orientation of the aromatic substituent

on the imine nitrogen atoms found in the solid state is maintained in solution. The aryl substituents with high steric demands (*ortho* substituents) have a lack of rotational freedom relative to the naphthalene backbone on the NMR time scale and exhibit well-resolved signals [24]. In **2**, a new band is observed at 1.2 ppm, assigned to the acetate groups. This band is slightly shifted (normally observed around 2 ppm) because of the shielding effect of the aromatic groups of the Pr-BIAN ligand. Assignments of the resonance in the ¹³C NMR spectra were made by using the APT pulse sequence and ¹H–¹³C-HETCOR spectroscopy of Pr-BIAN. This correlation spectrum directly allows assignment of the signals at 123.5, 127.7 and 128.7 ppm to C2, C3 and C4, respectively. Furthermore, assignment of the signals at 123.3 and 123.1 ppm to C15 and C16 is confirmed by their coupling with the signal at 7.26 ppm in the ¹H NMR [12]. The results show also that both ¹H and ¹³C NMR signals of the free Pr-BIAN ligand are shifted to higher frequency upon coordination to the metal center (Table 4). In complexes **2** and **4** new signals observed at 7.37 and 7.38 ppm, respectively, are assigned to H15', H16' and H17' and confirm the presence of two Pr-BIAN ligands coordinated to the metal center.

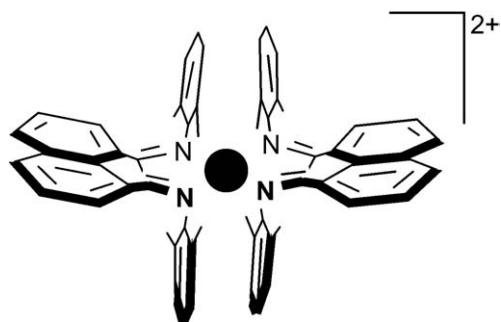


Fig. 2. Supposed structure of [Ni(Pr-BIAN)₂]²⁺ (**4**).

Table 4
¹H NMR data of Pr-BIAN free ligand and complexes (2) and (4)

	H23	H24	H22	H2	H15, H16, H17	H15', H16', H17'	H3	H3'	H4
	(d)	(d)	(sept)	(d)	(s)	(s)	(pst)	(pst)	(d)
Pr-BIAN	0.97	1.23	3.04	6.64	7.26	–	7.36	–	7.87
Complex (2)	1.02	1.29	2.96	6.91	7.37	7.40	7.48	7.63	8.29
Complex (4)	1.02	1.27	2.95	6.91	7.38	7.40	7.48	7.63	8.30

Abbreviations used, s = singlet, d = doublet, pst = pseudo triplet, sept = septet.

Table 5
¹³C NMR data of Pr-BIAN free ligand and complexes (2) and (4)

	C23	C24	C22	C2	C15, C17	C16	C3	C4	C5	C4, C18	C10	C13	C11
Pr-BIAN	23.1	23.4	28.6	123.5	123.3	124.1	127.7	128.7	129.3	130.9	140.6	147.3	160.7
Complex (2)	23.1	23.3	29.2	124.4	124.7	126.9	128.8	129.3	131.0	134.3	–	–	162.6
Complex (4)	23.1	23.3	29.2	124.4	–	126.9	128.7	129.3	131.0	134.3	–	–	162.6

Table 6
Antimicrobial and antimycotic activities in terms of MIC (mg ml⁻¹) after 48 h

Compound number	<i>S. aureus</i>	<i>E. coli</i>	<i>C. albicans</i>
Pr-BIAN	2.1	2.0	2.3
5	2.4	2.2	2.6
1	1.9	1.7	2.1
2	2.0	1.9	2.2
4	2.2	2.0	2.5
Ampicillin	2.0	1.9	
Streptomycin	2.5	2.1	
Clotrimazole			1.3
Nystatin			2.5

(18 mm against *E. coli*, 15 mm against *S. aureus* and 14 mm against *C. albicans*) and its cobalt complex **1** (22 mm against *E. coli*, 17 mm against *S. aureus* and 16 against *C. albicans*), which proved to possess remarkable activity against *S. aureus*, *E. coli* and *C. albicans*. On the other hand, the ligand **6** was void of antimicrobial activity. Minimum inhibitory concentration (MIC) [25] was determined for each of the active compounds along with ampicillin, streptomycin, clotrimazole and nystatin as standard controls; results are shown in Table 1. Amongst all the compounds tested, **Pr-BIAN**, **1** and **2** demonstrated the most potent antimicrobial activity against *S. aureus*, *E. coli* and *C. albicans*. It is noteworthy that the observed antimicrobial activity was highly dependent on the bulkiness of the *N*-bisimine derivatives, in which *ortho*-disubstituents played an important role in achieving an excellent level of biological activity. The 2,6-diisopropylphenyl groups represent the *N*-substituents of choice for the Schiff base in regard to antimicrobial induction. It is observed from these studies that metal chelates have a higher activity than the free ligand. Such increased activity of the metal chelates can be explained on the basis of Overtone's concept and chelation theory [26]. According to Overtone's concept of cell permeability the lipid membrane that surrounds the cell favors the passage of only lipid soluble materials due to which liposolubility is an important factor that controls antimicrobial activity. On chelation, the polarity of the metal ion is reduced to a greater extent due to the overlap of the ligand orbital and partial sharing of the positive charge of the metal ion with donor groups. Further, it increases the delocalization of *p*-electrons over the whole chelate ring and enhances the lipophilicity of the complex. This increased lipophilicity enhances the penetration of the complexes into lipid membranes and

blocking of metal binding sites on the enzymes of the microorganism. Attempts were made to correlate the antimicrobial activities of free ligands to Clog *P* (where Clog *P* is the calculated logarithm of partition coefficient) [27]. However, direct correlation could be established between Clog *P* and the antimicrobial activity of the free ligands, such as the Clog *P* value of **Pr-BIAN** (12.3) with MIC value of 2.0 µg ml⁻¹ against *E. coli* while the Clog *P* value of compound **5** (9.6) with MIC value of 2.2 µg ml⁻¹ against *E. coli* (Table 6).

2.5. Molecular modeling study of the free ligands *Pr-BIAN*, **6** and complex **1**

An attempt to gain a better insight on the molecular structures of the most active complex **1** and its free ligand **Pr-BIAN**, compared with the inactive ligand **6**, conformational analysis of the target compounds has been performed by the use of MM+ [28] forcefield as implemented in hyperchem 5.1 [29]. The starting atomic coordinates of the target compounds were obtained from the X-ray data of the **Pr-BIAN** and **6** [12]. The results show that the lowest energy conformer as calculated by PM3 semiempirical method [30] of both **Pr-BIAN** and **6** have approximate atomic coordinates with their X-ray data, respectively (Fig. 3). The calculations performed on **Pr-BIAN** indicate that the diaryl groups, showing highly free rotations, were spatially arranged itself approximately coplanar and perpendicular to the plane of acenaphthene core in face-to-edge arrangement in which the torsion angle ∠C2–N2–C6–C7 was 91.0°. This unique arrangement may be stabilized by three nonbonded interaction; CH/N interaction [13] (2.4 Å), intramolecular Face-to-edge aromatic interaction [14] (2.68 Å) and CH/π interaction [31] of isopropyl group with acenaphthene ring (2.87 Å). This nonbonded interaction may be the reason for the coplanarity of the diaryl groups and these three factors may be strong enough to compensate the steric repulsion. On the contrary, the calculation on **6**, diaryl groups were arranged itself perpendicular to the plane of acenaphthene with face to edge interaction and are not in the plane of the imine N-bond but make an angle ∠C2–N2–C6–C7 of 61.4° to it. This non-coplanar orientation of *p*-tolyl substituent is caused by the presence of naphthalene backbone, which prevents rotation of *p*-tolyl substituent in the plane formed by the imine function. Moreover, It is noteworthy to say that the PM3 calcula-

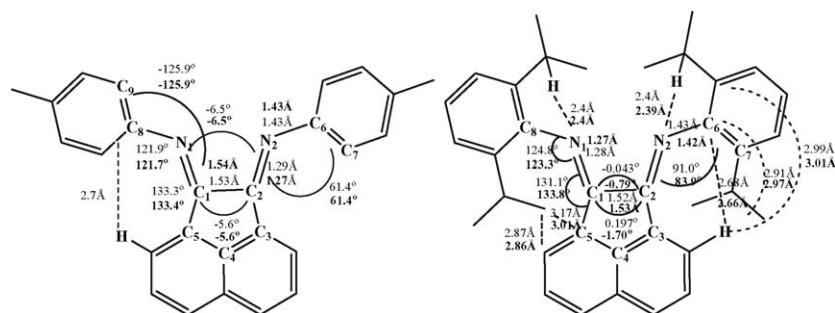


Fig. 3. Lowest PM3 minimized conformer of ligands **Pr-BIAN** and **6** (data in bold are the X-ray data).

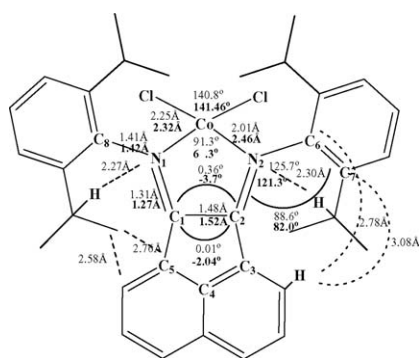


Fig. 4. Lowest ZINDO/1 minimized conformer of complex **1** (data in bold are the X-ray data of $[\text{Hg}(\text{Pr-BIAN})\text{Cl}_2]$ complex).

tion gives good result which is in a good agreement with the X-ray data compared with MM+ forcefield in which the angle $\angle\text{C2-N2-C6-C7}$ was overestimated 72° while underestimated 50° with AM1 [32] semiempirical molecular orbital. Similarly, conformational analysis of complex **1** using semiempirical ZINDO/1 calculation [33] afforded one conformation which has almost identical atomic coordinate with the analogous $[\text{Hg}(\text{Pr-BIAN})\text{Cl}_2]$ complex [34] (Fig. 4). This calculation showed tetrahedral geometry with the angle $\angle\text{Cl-Co-Cl}$ and the average N-Co bond length, are of 140.8 and 2.01 Å, respectively. A comparison with **Pr-BIAN** free ligand shows more planar *bis*(imino)acenaphthene skeleton as confirmed by smaller torsion angles, $\angle\text{N1-C1-C2-N2}$ of 0.36° and $\angle\text{C3-C2-C1-C5}$ of 0.01° . The corresponding angles of

Pr-BIAN ligand are -0.79° and -1.70° , respectively. The angle between the planes of naphthalene backbone and the aromatic *N*-substituents, $\angle\text{C2-N2-C6-C7}$, is more perpendicular in **1** (about 88.6°) than in the free **Pr-BIAN** ligand (about 76°). This must be ascribed to the *o*-isopropyl substituents on the aromatic groups, rather than to the coordination to cobalt. Moreover, complex **1** showed the same pattern of nonbonded interaction as described with **Pr-BIAN**.

The most stable conformers of complex **1** and free ligand **Pr-BIAN** resulting from computational chemistry analysis as a representative example, and the lowest energy conformer of the inactive ligand **6** were superimposed in order to reveal the similarities and differences in structure (Fig. 5). The strategy of overlay fit was match acenaphthene rings and examines any spatial differences between the atoms of the aryl groups. As a result of overlay of complex **1** and free ligand **Pr-BIAN** the atoms of the aryl groups occupy very slight different spatial position and perpendicular to the plane of acenaphthene ring. While overlay of both **Pr-BIAN** and **6** show that the atoms of the aryl groups occupy much different spatial position. In an attempt to understand the enhanced antimicrobial activity of **1** and **Pr-BIAN** compared with the **6**, electrostatic isopotential isosurface has been carried out for the lowest energy conformer of **1**, **Pr-BIAN** and **6** respectively, to examine the similarity in electronic and conformational properties. Fig. 6 presents the electrostatic potentials (ESP) mapped on the isosurface of the most biologically active **1** and **Pr-BIAN** and compared with inactive ligand **6**. Pink

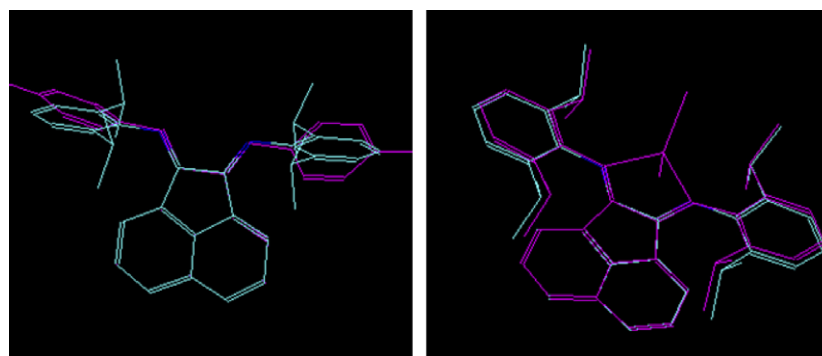


Fig. 5. Superimposition of low energy conformers of **Pr-BIAN** (cyan) with **6** (left; violet) and complex **1** (right; pink), respectively, and the corresponding root means squares (RMS) values showing the close match of both **Pr-BIAN** and complex **1**.

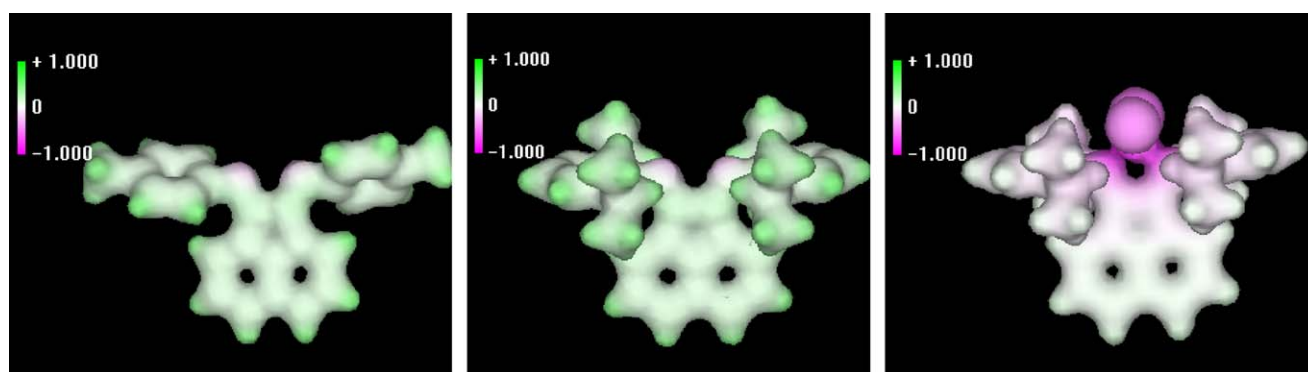


Fig. 6. Electrostatic potential isosurface of the lowest energy conformers of **6** (left), **Pr-BIAN** (middle) and **1** (right), negative region colors pink and positive region colors green.

colors indicate negative ESP regions and green colors indicate positive ESP regions. Comparison of the ESP of **1** and **Pr-BIAN** shows that increased negative charge regions located on the bisimine and on the center of coordinating metal in comparison with ligand **6**. Moreover, the occurrence of strong hydrophobic part represented by *bis* (*ortho*-disubstituents) in both **1** and **Pr-BIAN** indicating structural similarity and so on similar biological activity as evident from the experimental data.

3. Conclusion

We successfully prepared novel cobalt and Nickel complexes of *bis* [*N*-(2,6-diisopropylphenyl)imino] acenaphthene. These complexes, [Co(Pr-BIAN)Cl₂] **1**, [Co(OAc)₂(Pr-BIAN)₂](ClO₄) **2**, [Ni(Pr-BIAN)(NO₃)₂] **3** and [Ni(Pr-BIAN)₂](ClO₄)₂ **4**, have evaluated for their antimicrobial activity in comparison with the free ligands **Pr-BIAN**, **5** and **6**. Conformational analysis of the most active molecules **1** and its free ligand **Pr-BIAN** were performed using MM+ calculations and fully optimized with semiempirical PM3 [13] and ZINDO/1 [14] molecular orbital calculations. These semiempirical molecular orbital calculations give the most consistent results with experimental data for **Pr-BIAN** and its Mercuric complex.

4. Experimental

4.1. Instrumentation and materials

All starting materials were purchased from Wako Pure Chemical Industries Ltd., and used without further purification. Elemental analyses (C, H, N) were performed on a Perkin–Elmer 2400 Series II Analyzer. Electronic spectra were recorded on a UV-3100PC Shimadzu spectrophotometer using 10 mm pass length quartz cells at room temperature. Powder reflectance spectra were obtained using the same instrument equipped with an integrating sphere and using BaSO₄ as a reference. Infrared spectra were recorded on a Perkin–Elmer FT-IR Spectrometer 2000 as KBr pellets and as Nujol mulls in the 4000–370 cm^{−1} spectral range. Conductivity measurements were done on a TOA CM-40G EC instrument. ¹H and ¹³C NMR measurements at room temperature were obtained on a Jeol JNM LA 300 WB spectrometer at 400 MHz, using a 5 mm probe head in CDCl₃. Chemical shifts are given in ppm relative to internal TMS (tetramethylsilane). Full geometry optimization has been carried out for the most stable conformer with semiempirical PM3 [13] and ZINDO/1 [14] as implemented in Hyperchem 5.1 running on PC. The Eigenvector Following (EF) routine was used for optimizer. Calculation of the isopotential molecular surface was performed with HyperChem 5.1.

4.2. Synthesis of metal complexes

4.2.1. [Co(Pr-BIAN)Cl₂] (**1**, C₃₆H₄₀Cl₂CoN₂)

CoCl₂·6H₂O (0.18 g, 0.74 mmol) and Pr-BIAN (0.37 g, 0.74 mmol) were mixed in ethanol/acetic acid (3:1 volume

ratio). After 2 h of stirring at room temperature, the dark-bluish green powder obtained was filtered, washed with ethanol followed by *n*-hexane and dried in vacuo. Yield, 0.37 g (79%).

4.2.2. [Co(OAc)₂(Pr-BIAN)₂](ClO₄) (**2**, C₇₆H₈₆ClCoN₄O₈)

Co(ClO₄)₂·6H₂O (0.135 g, 0.37 mmol) was dissolved in 20 ml methanol and added to 10 ml of a chloroform solution of Pr-BIAN 0.37 g (0.74 mmol). To this solution was added 5 ml of acetic acid and the mixture was stirred at room temperature. After 3 h of stirring a red powder product could be obtained. This solid was filtered, washed with methanol followed by *n*-hexane and dried in vacuo. Yield, 0.34 g (70%).

4.2.3. [Ni(Pr-BIAN)(NO₃)₂] (**3**, C₃₆H₄₀N₄NiO₆)

Ni(NO₃)₂·6H₂O (0.14 g, 0.5 mmol) and Pr-BIAN 0.25 g (0.5 mmol) were mixed in 30 ml ethanol. After 4 h of stirring at room temperature, the formed dark-green powder product was filtered, washed with ethanol followed by *n*-hexane and dried in vacuo. Yield, 0.37 g (79%).

4.2.4. [Ni(Pr-BIAN)₂](ClO₄)₂ (**4**, C₇₂H₈₀Cl₂N₄NiO₈)

Ni(ClO₄)₂·6H₂O (0.27 g, 0.74 mmol) and Pr-BIAN 0.74 g (1.48 mmol) were mixed and 30 ml of acetic acid was added. After 4 h of stirring at room temperature, the red powder product was filtered, washed with *n*-hexane and dried in vacuo. Yield, 0.80 g (86%).

4.3. Antimicrobial testing

The antimicrobial screening of all the synthesized compounds was done using cup diffusion technique. This screening was performed against the Gram-negative *Pseudomonas aeruginosa* and *Escherichia coli* and the Gram-positive *Staphylococcus aureus* and *Bacillus subtilis*, in addition to the pathogenic fungi *Candida albicans*. The following standard organisms used in the antimicrobial screening were obtained from IFO (Institute Fermentation of Osaka); *P. aeruginosa* IFO 3448, *E. coli* IFO 3301, *S. aureus* IFO 3060, *B. subtilis* IFO 3007 and *C. albicans* IFO 0583. From the inhibition zone diameter data analysis, both free ligands and their metal complexes exhibited considerable antimicrobial activity against *S. aureus*, *E. coli* and *C. albicans* (Table 1). The tested compounds were dissolved in dimethylsulfoxide (DMSO) at a concentration of 1 mg ml^{−1}. The suitable medium (nutrient agar for bacteria and Sabouraud agar for fungi) was inoculated with the test organisms. An aliquot of the solution of each the test compounds equivalent to 100 µg was placed separately in cups, cut in the agar. The plates were incubated at 37 °C for 18–24 h for bacteria and 48 h for *C. albicans*, and the resulting inhibition zones were measured. DMSO, which exhibited no antimicrobial activity against the test organisms, was used as a negative control. Minimal inhibitory concentration (MIC) was determined using the broth dilution technique. Ampicillin, streptomycin, clotrimazole and nystatin were used during the test procedure as reference antibiotics.

Acknowledgements

The authors would like to Mr. Shady Kamal (Department of Microbiology, Faculty of Pharmacy, Mansoura University, Egypt) for providing the antibacterial data.

References

- [1] K.Y. Lau, A. Mayr, K.K. Cheung, *Inorg. Chim. Acta* 285 (1999) 223.
- [2] A.S. Shawali, N.M.S. Harb, K.O. Badahdah, *J. Heterocyclic Chem.* 22 (1985) 1397.
- [3] V. Opletalová, J. Hartl, A. Patel, A. Palát, V. Buchta, *Farmaco* 57 (2002) 135.
- [4] M. Biava, R. Fioravanti, G.C. Porretta, G. Sleite, D. Deidda, G. Lampis, R. Pompei, *Farmaco* 54 (2002) 721.
- [5] Z. Travnicek, M. Malon, Z. Sindelar, K. Dolezal, J. Rolcik, V. Krystof, M. Strnad, J. Marek, *J. Inorg. Biochem.* 84 (2001) 23.
- [6] J.H. Groen, C.J. Elsevier, K. Vrieze, W.J.J. Smeets, A.L. Spek, *Organometallics* 15 (1996) 3445.
- [7] J.H. Groen, J.G.P. Delis, P.W.N.M. van Leeuwen, K. Vrieze, *Organometallics* 16 (1997) 68.
- [8] J.G.P. Delis, J.H. Groen, K. Vrieze, P.W.N.M. van Leeuwen, N. Veldman, A.L. Spek, *Organometallics* 16 (1997) 551.
- [9] J.H. Groen, M.J.M. Vlaar, P.W.N.M. van Leeuwen, K. Vrieze, H. Kooijman, A.L. Spek, *J. Organomet. Chem.* 551 (1998) 67.
- [10] U. El-Ayaan, A. Paulovicova, S. Yamada, Y. Fukuda, *J. Coord. Chem.* 56 (2003) 373.
- [11] U. El-Ayaan, F. Murata, S. El-Derby, Y. Fukuda, *J. Mol. Str.* 692 (2004) 209.
- [12] R. van Asselt, C.J. Elsevier, W.J.J. Smeets, L. Spek, R. Benedix, *Recl. Trav. Chim. Pays Bas* 113 (1994) 88.
- [13] M. Eto, K. Setoguchi, A. Harada, E. Sugiyama, K. Harano, *Tetrahedron Lett.* 39 (1998) 9751.
- [14] Y. Yoshitake, H. Nakagawa, M. Eto, K. Harano, *Tetrahedron* 56 (2000) 6015.
- [15] W.J. Geary, *Coord. Chem. Rev.* 7 (1971) 81.
- [16] K. Nakamoto, *Infrared Spectra of Inorganic and Coordination Compounds*, second ed, Wiley-Interscience, New York, 1970.
- [17] Y. Ihara, Y. Fukuda, K. Sone, *Bull. Chem. Soc. Jpn.* 59 (1986) 1825.
- [18] Y. Fukuda, C. Fujita, H. Miyamae, H. Nakagawa, K. Sone, *Bull. Chem. Soc. Jpn.* 62 (1989) 745.
- [19] Y. Fukuda, R. Morishita, K. Sone, *Bull. Chem. Soc. Jpn.* 49 (1976) 1017.
- [20] P. Chaudhuri, M. Winter, U. Flörke, H.-J. Haupt, *Inorg. Chim. Acta* 232 (1995) 125.
- [21] M. Burke-Laing, M. Laing, *Acta. Crystallogr. Sect. B* 32 (1976) 3216.
- [22] A. Paulovicova, U. El-Ayaan, K. Umezawa, C. Vithana, Y. Ohashi, Y. Fukuda, *Inorg. Chim. Acta* 339 (2002) 209.
- [23] A.B.P. Lever, *Inorganic Electronic Spectroscopy*, 2nd Ed, Elsevier, New York, 1984.
- [24] A.K. Gushurst, D.R. McMillin, C.O. Dietrich-Buchecker, P.A. Marriot, J.-P. Sauvage, *Inorg. Chem.* 28 (1989) 4070.
- [25] R.N. Jones, A.L. Barry, T.L. Gavan, I.I.J.A. Washington, in: E.H. Lennette, A. Ballows, W.J. Hausler, H.J. Shadomy (Eds.), *Manual of Clinical Microbiology*, American Society for microbiology, Washington DC, 1985, pp. 972 (4th edn).
- [26] N. Raman, V. Muthuraj, S. Ravichandran, A. Kulandaisamy, *Proc Indian Acad Sci.* 115 (2003) 161.
- [27] Calculated logP (ClogP) values were computed by using the CS ChemDraw Ultra ver.7.0, by CambridgeSoft.Com, Cambridge, MA, USA, 2001 (November 27).
- [28] N.L. Allinger, *J. Am. Chem. Soc.* 99 (1977) 8127.
- [29] HyperChem version 5.1 Hypercube, Inc.
- [30] J.J.P. Stewart, *J. Comput. Chem.* 2 (1989) 209.
- [31] Y. Umezawa, S. Tsuboyama, H. Takahashi, J. Uzawa, M. Nishio, *Tetrahedron* 55 (1999) 10047.
- [32] M.J.S. Dewar, E.G. Zoebisch, E.F. Healy, J.J.P. Stewart, *J. Am. Chem. Soc.* 107 (1985) 3902.
- [33] A.D. Bacon, M.C. Zerner, *Theor. Chim. Acta* 53 (1979) 21.
- [34] U. El-Ayaan, *Monat. Chem.* 135 (2004) 919.